

September 2018

Origins of ultradiffuse galaxies in the Coma cluster – I. Constraints from velocity phase space

Adebusola Alabi
University of California Observatories

Anna Ferré-Mateu
Swinburne University of Technology

Aaron Romanowsky
San Jose State University

Jean Brodie
University of California Observatories

Duncan Forbes
Swinburne University of Technology

See next page for additional authors

Follow this and additional works at: https://scholarworks.sjsu.edu/physics_astron_pub



Part of the [External Galaxies Commons](#), and the [Stars, Interstellar Medium and the Galaxy Commons](#)

Recommended Citation

Adebusola Alabi, Anna Ferré-Mateu, Aaron Romanowsky, Jean Brodie, Duncan Forbes, Asher Wasserman, Sabine Bellstedt, Ignacio Martín-Navarro, Viraj Pandya, Maria Stone, and Nobuhiro Okabe. "Origins of ultradiffuse galaxies in the Coma cluster – I. Constraints from velocity phase space" *Monthly Notices of the Royal Astronomical Society* (2018): 3308-3318. <https://doi.org/10.1093/mnras/sty1616>

This Article is brought to you for free and open access by the Physics and Astronomy at SJSU ScholarWorks. It has been accepted for inclusion in Faculty Publications by an authorized administrator of SJSU ScholarWorks. For more information, please contact scholarworks@sjsu.edu.

Authors

Adebusola Alabi, Anna Ferré-Mateu, Aaron Romanowsky, Jean Brodie, Duncan Forbes, Asher Wasserman, Sabine Bellstedt, Ignacio Martín-Navarro, Viraj Pandya, Maria Stone, and Nobuhiro Okabe

Origins of ultradiffuse galaxies in the Coma cluster – I. Constraints from velocity phase space

Adebusola Alabi,¹ Anna Ferré-Mateu,² Aaron J. Romanowsky,^{1,3} Jean Brodie,¹ Duncan A. Forbes,² Asher Wasserman,¹ Sabine Bellstedt,² Ignacio Martín-Navarro,¹ Viraj Pandya,¹ Maria B. Stone^{3,4} and Nobuhiro Okabe^{5,6,7}

¹University of California Observatories, 1156 High St, Santa Cruz, CA 95064, USA

²Centre for Astrophysics & Supercomputing, Swinburne University of Technology, Hawthorn VIC 3122, Australia

³Department of Physics and Astronomy, San José State University, San Jose, CA 95192, USA

⁴Department of Physics and Astronomy, University of Turku, FI-20014, Finland

⁵Department of Physical Science, Hiroshima University, 1-3-1, Kagamiyama, Higashi-Hiroshima, Hiroshima 739-8526, Japan

⁶Hiroshima Astrophysical Science Center, Hiroshima University, 1-3-1, Kagamiyama, Higashi-Hiroshima, Hiroshima 739-8526, Japan

⁷Core Research for Energetic Universe, Hiroshima University, 1-3-1, Kagamiyama, Higashi-Hiroshima, Hiroshima 739-8526, Japan

Accepted 2018 June 15. Received 2018 May 23; in original form 2018 January 27

ABSTRACT

We use Keck/DEIMOS spectroscopy to confirm the cluster membership of 16 ultradiffuse galaxies (UDGs) in the Coma cluster, bringing the total number of spectroscopically confirmed UDGs from the Yagi et al. (Y16) catalogue to 25. We also identify a new cluster background UDG, confirming that most (~ 95 per cent) of the UDGs in the Y16 catalogue belong to the Coma cluster. In this pilot study of Coma UDGs in velocity phase space, we find evidence of a diverse origin for Coma cluster UDGs, similar to normal dwarf galaxies. Some UDGs in our sample are consistent with being late infalls into the cluster environment, while some may have been in the cluster for ≥ 8 Gyr. The late infallen UDGs have higher absolute relative line-of-sight velocities, bluer optical colours, and within the projected cluster core, are smaller in size, compared to the early infalls. The early infall UDGs, which may also have formed *in situ*, have been in the cluster environment for as long as the most luminous galaxies in the Coma cluster, and they may be failed galaxies that experienced star formation quenching at earlier epochs.

Key words: galaxies: dwarf – galaxies: evolution – galaxies: interactions – galaxies: kinematics and dynamics.

1 INTRODUCTION

One of the overarching challenges that has attended the discovery of ultradiffuse galaxies (UDGs) is properly reconciling their observed properties with the various scenarios that have been advanced for their formation. UDGs, which have now been found in diverse environments (e.g. van Dokkum et al. 2015; van der Burg, Muzzin & Hoekstra 2016; Janssens et al. 2017; Román & Trujillo 2017b; van der Burg et al. 2017), have low surface brightness (LSB; ≥ 24 mag arcsec⁻²), sizes that are comparable to or even larger than L^* ellipticals, luminosities consistent with dwarf galaxies ($\sim 10^8 L_\odot$) but in some cases, associated with massive halos. They have also been successfully identified in cosmological simulations (e.g. Chan et al. 2017; Di Cintio et al. 2017; Rong et al. 2017). The two major scenarios that attempt to explain the origin of UDGs describe

them either as failed galaxies or puffy dwarfs, with both emerging paradigms increasingly finding support from observations.

For example, initial studies of the spatial distribution (e.g. van der Burg et al. 2016; Román & Trujillo 2017a), colours (e.g. Beasley & Trujillo 2016; Yagi et al. 2016), and the shapes (Burkert 2017) of UDGs in dense environments point at a similarity to dwarfs, while the formation landscape is ill-defined when one considers the central velocity dispersion (van Dokkum et al. 2016), the stellar populations, and the globular cluster systems in the handful of UDGs so far studied. It appears that UDGs in dense environments may be dominated by intermediate-to-old and metal-poor stellar populations (e.g. Gu et al. 2017; Kadowaki, Zaritsky & Donnerstein 2017; Pandya et al. 2017), while in less-dense environments, some UDGs have been shown to host younger stellar populations (e.g. DGSAT I Pandya et al. 2017 and the UDGs in the Hickson Compact groups Shi et al. 2017; Spekkens & Karunakaran 2017, respectively), with hints of an extended star formation history.

* E-mail: aalabi@ucsc.edu

Results from complementary studies of the globular cluster systems associated with UDGs reveal populations that are indicative of either dwarfs or L^* galaxies (Beasley & Trujillo 2016; DF17 with 27 GCs; see also van Dokkum et al. 2017; Amorisco et al. 2018; DF44 and DFX1 with ~ 74 and ~ 62 GCs, respectively).

It may be possible to gain clearer insights into the origin of UDGs by studying them in velocity phase space (Bertschinger 1985; Mamon et al. 2004; Mahajan, Mamon & Raychaudhury 2011; Oman, Hudson & Behroozi 2013; Haines et al. 2015; Vijayaraghavan, Gallagher & Ricker 2015; Rhee et al. 2017). Conselice, Gallagher & Wyse (2001) used the velocity phase-space analysis to show the late accretion origin of the dwarf galaxy population in the Virgo cluster, relative to the cluster giants. Recently, accreted groups of galaxies that are yet to be completely disrupted within the cluster potential may still retain a memory of their origins, showing up as ‘lumps’ or ‘streams’ around some giant galaxies. Mendelin & Binggeli (2017) recently found a significant excess of faint galaxies around giant spiral galaxies in the Coma cluster, mostly at large clustercentric radii and explained their result as evidence of the hierarchical build-up of the cluster.

For a Coma-sized cluster, where the relaxation and energy equipartition time-scales are significantly longer than the Hubble time ($> 2.63 \times 10^{11}$ Gyr, using equation 7.1 from Binney & Tremaine 2008 and ~ 22 Gyr, considering only the most massive galaxies and using equation 2.36 from Sarazin 1986, respectively), it is reasonable to explore phase space for evidence in support of or against the recent infall hypothesis. To first order, galaxies populate distinct phase-space regions according to their accretion epochs, with their radial velocities reflecting the cluster mass at infall. UDGs (and other cluster galaxies) accreted at earlier epochs should be virialized. These galaxies would have experienced the quenching effects of the various physical processes operating within the cluster environments for a longer time, and they should have passively evolved to be maximally red in optical colours. Recent infalling UDGs, on the other hand, are expected to have higher velocities, reflecting the cluster mass at infall and to be bluer (in a standard dwarf-like picture).

Phase-space exploration of UDGs is, however, challenging and expensive primarily due to their faintness. Even in a UDG-rich environment, such as the Coma cluster, which may host ~ 200 – 300 UDGs (Yagi et al. 2016, hereafter Y16, and Janssens et al. 2017), only 10 of them have been spectroscopically confirmed (van Dokkum et al. 2016; Gu et al. 2017; Kadowaki et al. 2017; van Dokkum et al. 2017; Ruiz-Lara et al. 2018) from a combined ≥ 54 h of observation, mostly with 10-m class telescopes. Apart from the intrinsic faintness of UDGs, the relative proximity of the Coma cluster at ~ 100 Mpc, and thus its angular extent of $\geq 2^\circ$ on the sky, makes an attempt to obtain a large representative sample of UDG radial velocities extremely time consuming. Nevertheless, in this paper, we report the spectroscopic confirmation of 16 new UDGs in the Coma cluster and test the recent infall hypothesis by comparing UDG kinematics with other cluster galaxy populations. This paper is the first in a series based on new Keck/DEIMOS data that seek to understand the origins of UDGs in cluster environments. The reader is referred to F erre-Mateu et al. (2018, hereafter Paper II) for a detailed study of the stellar populations of a subsample of the UDGs studied here.

The outline of the paper is as follows: Section 2 describes our sample selection, observational set-up, and data reduction methodology. In Section 3, we present our radial velocity measurements. In Section 4, we use our results to address some fundamental questions about the origins of UDGs in cluster environments.

Throughout this work, we adopt a distance of 100 Mpc, a virial radius of ~ 2.9 Mpc, and a virial mass of $\sim 2.7 \times 10^{15} M_\odot$ for the Coma cluster (Kubo et al. 2007). We use a mean heliocentric radial velocity of 6943 km s^{-1} , a central velocity dispersion of 1031 km s^{-1} , and central co-ordinates RA: 12:59:48.75 and Dec.: +27:58:50.9 for the Coma cluster (Makarov et al. 2014). Lastly, we adopt the following cosmology: $\Omega_m = 0.3$, $\Omega_\Lambda = 0.7$, and $H_0 = 70 \text{ km s}^{-1} \text{ Mpc}^{-1}$.

2 DATA: SAMPLE SELECTION, OBSERVATIONS, AND REDUCTION

2.1 Sample Selection

We obtained spectroscopic data for a sample of Coma cluster LSB galaxies from the Subaru–LSB catalogue of Y16 (see Fig. 1 for a montage of our LSB sample). It should be noted that most of the LSB galaxies from Y16 fall short of the UDG definition in van Dokkum et al. (2015), i.e. $R_e > 1.5 \text{ kpc}$ and $\mu_0 > 24 \text{ mag arcsec}^{-2}$, in the g -band (equivalent to $23.5 \text{ mag arcsec}^{-2}$ in the R -band). Therefore, we select 25 LSB galaxies from the Y16 catalogue that maximize the number of unambiguous UDGs and simultaneously include targets from the core and outskirts regions of the cluster. Our sample has six targets in common with the van Dokkum et al. (2015) catalogue: Yagi093 (DF26), Yagi276 (DF28), Yagi285 (DF25), Yagi364 (DF23), Yagi762 (DF36), and Yagi782 (DF32).

In Fig. 2, where we show the size–luminosity diagram of our target sample, most of our spectroscopic targets occupy a similar parameter space comparable to other Coma UDGs previously studied in the literature. Three galaxies in our sample (Yagi266, Yagi413, and Yagi772) are not consistent with the generally accepted definition of UDGs. A careful comparison of the sizes of the UDGs common to both Y16 and van Dokkum et al. (2015) shows that, on average, R_e from Y16 is ~ 15 per cent smaller than those reported in van Dokkum et al. (2015), hence we relax the UDG size criterion for the Y16 galaxies to $R_e > 1.3 \text{ kpc}$, and note that this size refers to the semimajor axis effective radius. This disparity in R_e could be due to differences in the image qualities or the galaxy size fitting techniques employed in both studies. Fig. 3 shows our spectroscopic targets in the plane of the sky. Unlike the spectroscopically confirmed Coma UDGs in the literature that are mostly at large projected clustercentric radii, our UDGs sample extends well into the cluster core.

2.2 Observations

Our spectroscopic data were obtained from the Keck II telescope with the DEIMOS spectrograph from 2017 April 27–29 during dark night conditions with a mean seeing of $0''.7$. We observed two DEIMOS masks, positioned at 0.4 Mpc in the south direction (central mask) and 1.6 Mpc in the south-west direction (outer mask), respectively, from the cluster centre. We set up DEIMOS with the GG455 filter and the 600 grating centred on 6000 \AA . This resulted in spectral data with resolution of 14 \AA (this corresponds to an instrumental resolution of 300 Km s^{-1}) and wavelength coverage spanning ~ 4300 – 9600 \AA , depending on the position of the slit on the masks. We integrated on the central mask for a total of 14.5 h over three nights and on the outer mask for a modest total time of 2 h, with individual exposures of 30 min. With the longer integration on the central mask, we also explore the stellar populations of these UDGs in a companion paper (see Paper II).

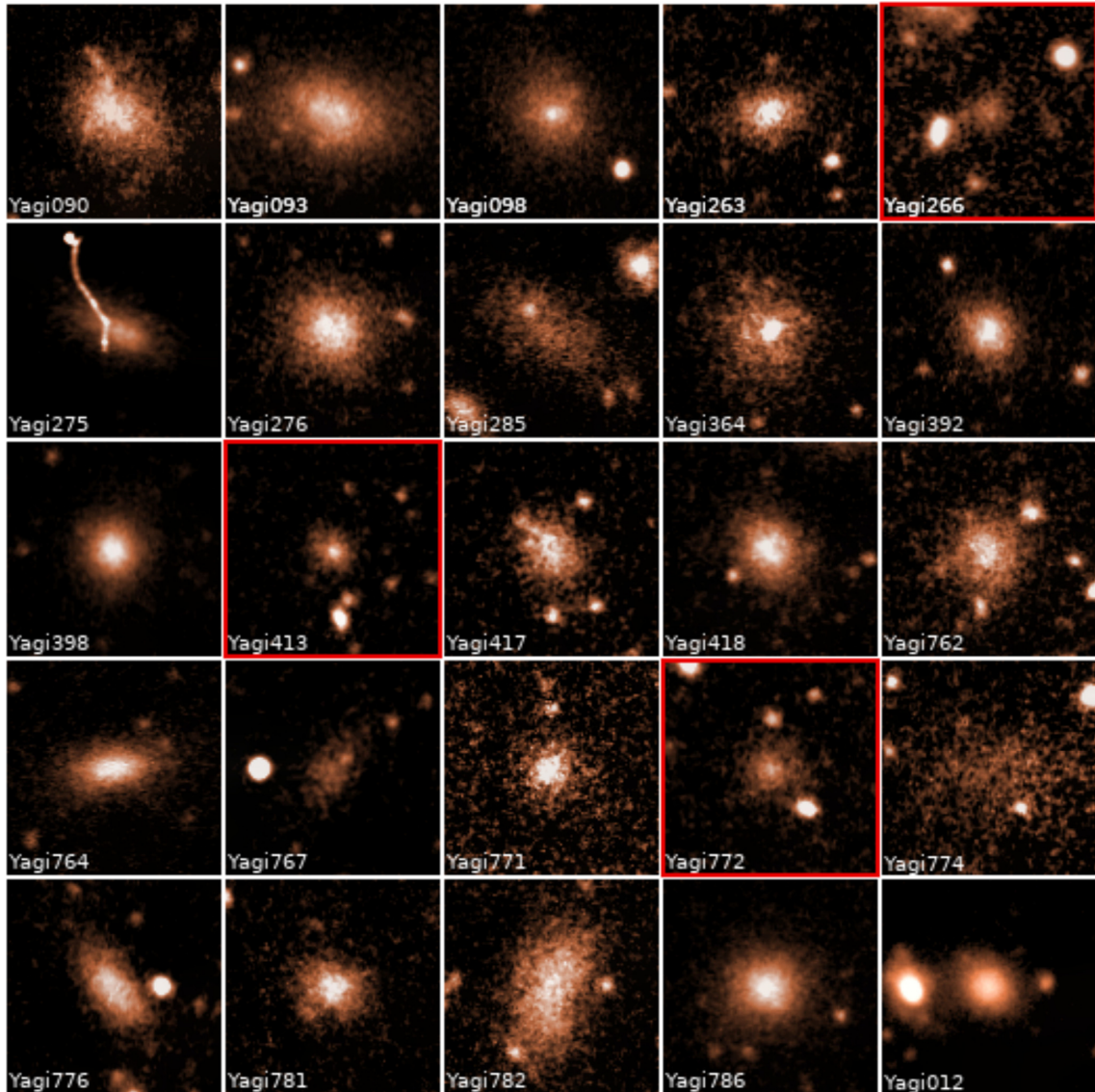


Figure 1. Thumbnails of the 25 Coma cluster LSB galaxies studied in this work, from V -band Suprime-Cam/Subaru imaging. Each thumbnail is 10×10 kpc across. North is up and east is to the left. Three of our LSB galaxies fail the $R_e > 1.5$ kpc criterion from van Dokkum et al. (2015), and they are not UDGs. These galaxies have been highlighted in the diagram with red borders. The galaxy IDs shown here are from the Coma LSB catalogue of Yagi et al. (2016). We report spectroscopic redshifts for 16 new Coma UDGs and a Coma cluster background galaxy in this work. The stream-like feature superimposed on Yagi 275 is an image flaw.

Our masks had custom slits that were 3 arcsec wide in order to capture as much UDG light as possible. In addition, we also increased the gaps between slits from the nominal $0''.7$ to 1 arcsec and avoided placing bright filler objects on adjacent slits to our UDG targets to prevent possible cross-talk across slits. These adjustments are based on trial observations we made in 2017 January. To summarize our masks based on their targets, the central mask had 12 UDG slits, 2 LSB slits, 8 dedicated sky slits, and 15 filler-object slits, while the outer mask had 9 UDG slits, 1 LSB slit, 5 dedicated sky slits, and 23 filler-object slits. We identified suitable filler objects from the field-of-view and placed slits on them so as not to waste any real estate on the masks. A few of these filler objects have been detected in the Sloan Digital Sky Survey (SDSS)

and have kinematics data available in the literature with which we compare our new velocity measurements.

2.3 Data Reduction

We reduced the data with a modified version of the IDL DEEP2 DEIMOS SPEC2D pipeline (Cooper et al. 2012) that accounts for the spatially diffuse nature of our targets and for proper sky subtraction. We performed two sets of data reduction on the central mask: one, where we combined the optimally extracted 1D spectra data from each night, and two, where we combined the 2D slit spectra from the data reduction process before extracting a single final 1D spectrum.

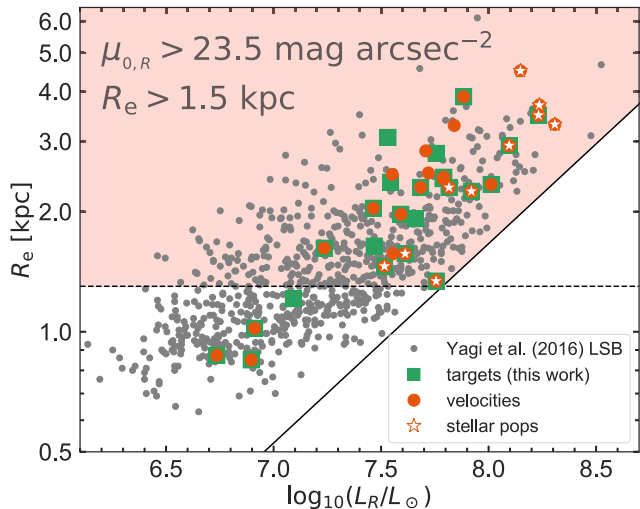


Figure 2. Size–luminosity diagram of our LSB spectroscopic galaxy sample. We have marked the 25 targets studied in this work (green squares), chosen from the Yagi et al. (2016) LSB catalogue (grey dots). Galaxies with radial velocities from this work and in the literature as well as those with stellar population parameters from Ferré-Mateu et al. (2018) and in the literature, have been marked as shown in the plot legend. The shaded region, defined by the dashed line, which corresponds to the $R_e > 1.5$ kpc criterion from van Dokkum et al. (2015), has been scaled to reflect that sizes from Yagi et al. (2016) are 15 per cent smaller than those of van Dokkum et al. (2015), and the slanted solid line, which is a line of constant mean surface brightness ($\mu_0 = 23.5$ mag arcsec $^{-2}$ in R -band), shows that most of our targets are consistent with the UDG definitions in the literature.

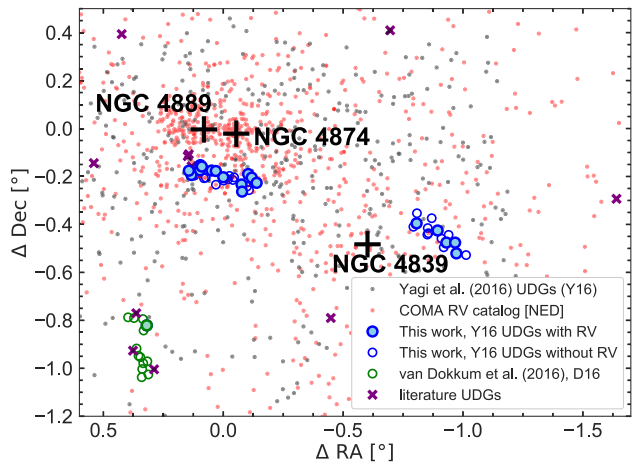


Figure 3. Spatial distribution of galaxies in the Coma cluster, highlighting the central and outer fields studied in this work. The solid crosses show the three most luminous galaxies within the cluster, while the grey dots are the UDGs from the Coma cluster–LSB catalogue of Yagi et al. (2016). The red dots are Coma cluster galaxies with radial velocity measurements available in the literature (sourced from NED). Spectroscopically confirmed Coma cluster UDGs from the literature are shown as purple crosses. The filled and open circles are the UDGs and non-UDGs, respectively, studied in this work for which we have successfully measured radial velocities. The green circles are from the DEIMOS observation (see Section 2.4 for more details) described in van Dokkum et al. (2016).

We do not observe any significant difference between the final 1D spectra from the two methods, and hence, we use the reduced data from the first approach in subsequent analyses.

2.4 Remarks on the D16 mask

As shown in Fig. 3, we have also supplemented our data with the non-UDG objects from the DEIMOS mask (D16) reported in van Dokkum et al. (2016, 2017). This mask was observed with the GG550 filter, the 1200 lines mm $^{-1}$ grating and a central wavelength of 6300 Å for a total of 33.5 h over two nights. The mask was designed primarily to observe four UDGs: two from the van Dokkum et al. (2015) catalogue, i.e. DF42 and DF44, and two additional UDGs from their *CFHT* imaging introduced in van Dokkum et al. (2017), i.e. DFX1 and DFX2. Note that DFX2 is also catalogued in Y16 as Yagi012. Apart from Yagi012, these UDGs all have their radial velocities published in van Dokkum et al. (2017). In addition, 33 slits were positioned on mask filler objects.

We reduced the entire mask as described in Section 2.3 except in this case, we perform local sky subtraction. While such sky subtraction might not be adequate for the UDGs on this mask due to their diffuse nature, however, the sole purpose of adding this mask is to obtain radial velocities for the non-UDG cluster galaxies near the UDGs.

3 RESULTS

3.1 Radial Velocities

The reduced 1D spectra from the central and outer masks have signal-to-noise ratio (SNR) ranging over 5–20 and 5–7 Å $^{-1}$, respectively. Owing to this modest SNR, we use the *FXCOR* package in *IRAF* to determine the radial velocities of our targets, though we also used the *REDUCEME/MIDEZ* package (Cardiel 1999) on the central mask to independently determine our radial velocities. Both methods returned radial velocities that are in excellent agreement. In *IRAF*, we cross-correlated our 1D spectra with stellar templates sourced from the new *MILES* (Vazdekis et al. 2016) spectral library (with full width at half-maximum of 14 Å), obtained the cross-correlation peak, and fitted it with a sinc function¹ to obtain the velocity estimates.

To obtain robust velocity estimates, we only consider outputs from *FXCOR* with the Tonry & Davis ratio (TDR parameter; Tonry & Davis 1979) ≥ 3 . This TDR parameter cut-off is equivalent to an SNR ≥ 5 limit. Furthermore, when both the H β and H α absorption features are observed in the spectral data, as is the case for 23 of the 62 science slits, we split the spectrum into two segments, i.e. ~ 4600 – 5100 and ~ 6400 – 6900 Å, respectively, and obtained independent estimates of the redshifts. We note that due to the relative brightness of the night sky, we are not able to use our reduced spectral data redward of 6900 Å. Fig. 4 shows the rest-frame spectra of two representative UDGs from both masks.

The offsets between these multiple velocity estimates vary between 10 and 450 km s $^{-1}$. We note that this is adequate for the purpose of determining the cluster membership of our targets and consistent with our spectral resolution. In Fig. 5, we show the agreement between the velocity estimates obtained from the H β - and

¹We also tried the cross-correlation using the parabolic function, but we only report results that are invariant to the fitted function.

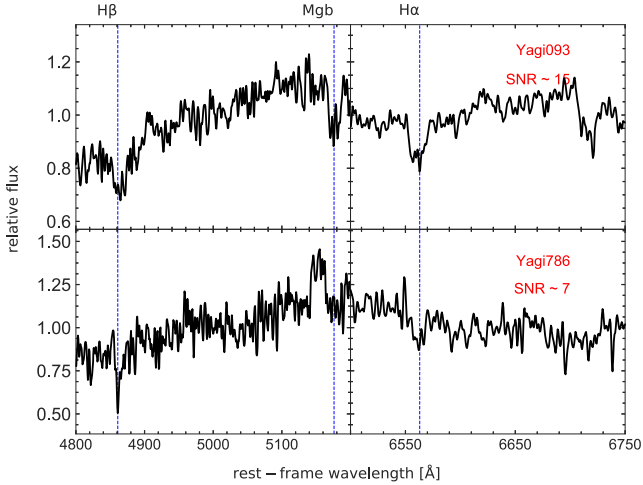


Figure 4. Rest-frame spectra of representative UDGs from the central and outer masks. In the *top* and *bottom* panels, we show the spectra of Yagi093 (central mask) and Yagi786 (outer mask), respectively, with the $H\beta$, Mgb , and $H\alpha$ spectral absorption features highlighted.

$H\alpha$ -spectral regions. For these targets, we adopt the weighted average of the $H\beta$ - and $H\alpha$ -determined velocities, weighting by the TDR parameter returned from `FXCOR`. Otherwise, we report velocity measurements made around the $H\beta$ region. We obtained uncertainties on our velocity measurements by summing in quadrature the `FXCOR` error and the standard deviation among the stellar templates. We are able to compare the radial velocities of Yagi 093, Yagi 418, and some filler objects with measurements available in the literature and show the generally good agreement in Fig. 5.

For our D16 mask, we successfully measured the radial velocities of 25 (including all the UDGs) of the 33 slit targets as described in Section 3.1, using only the $H\alpha$ -spectral region. We measured a radial velocity of 6473 km s^{-1} for Yagi 012 and similar velocities for the other UDGs as already published in the literature. The non-UDGs with radial velocities consistent with the Coma cluster are shown in Table 1.

3.2 Summary of results

We summarize our heliocentric-corrected radial velocity measurements, and other relevant data, in Table 1 and show the cluster-centric radial velocity distribution in Fig. 6. From this diagram, a few spectroscopically confirmed cluster galaxies in the cluster outskirts, both from our new measurements and our NASA/IPAC Extragalactic Database (NED)² compilation, have radial velocities that often deviate from the cluster velocity limits shown. These may be new infalls or back-splashing galaxies. We have obtained reliable radial velocity measurements for 19 of our original sample of 25 LSB galaxies, with 16 of them being *bona fide* UDGs, two smaller LSB galaxies, and one cluster background UDG, Yagi 771 (from the outer mask). Our velocity measurement puts it at ~ 60 Mpc behind the Coma cluster. This adds to the list of field UDGs with spectroscopic velocity measurements, the others being DGSAT I (Martínez-Delgado et al. 2016) and DF03 (Kadowaki et al. 2017). With only one of these 19 LSB galaxies qualifying as a background galaxy, we confirm that most of the galaxies in the Y16 catalogue,

i.e. ~ 95 per cent, are indeed Coma cluster members. We have updated the R_c value for Yagi 771 in Table 1 to reflect this new result. In addition, we confirm the cluster membership of Yagi 012 from the D16 mask. We have also obtained radial velocities for 35 non-UDG Coma cluster galaxies. Also, there are three UDGs (DF42, DF44, and Yagi 012) in the south-east direction of the cluster (see Fig. 3) that are within 320 kpc and 130 km s^{-1} of each other, and thus may represent a bound group of UDGs.

4 DISCUSSION

In this work, we have successfully measured the radial velocities of 16 UDGs, two LSB galaxies, and one background cluster galaxy from the Y16 Subaru-LSB catalogue. This brings the total number of spectroscopically confirmed Coma cluster UDGs from the Y16 LSB catalogue to 25 (see Gu et al. 2017; Kadowaki et al. 2017; van Dokkum et al. 2017; Ruiz-Lara et al. 2018) with the important addition that we now report spectroscopically confirmed UDGs within the projected cluster core, i.e. ≤ 0.5 Mpc. With our UDG kinematic data that span a wide clustercentric radial baseline, we now briefly address the following salient questions that should help provide more insights into the origins of UDGs in cluster environments.

4.1 Are UDGs kinematically distinct within the cluster?

As shown in Fig. 6, UDGs within the projected cluster core have a similar velocity range to other neighbouring galaxies along the line of sight. The UDGs with highest relative line-of-sight velocities within the core are linked with the deepest parts of the cluster gravitational potential well. The situation is a little nuanced for the UDGs at larger clustercentric radii since we do not have complete azimuthal coverage. The kinematics of the UDGs from our outer mask most likely reflect the peculiar local effect within the substructure centred on NGC 4839. This well-known substructure has been identified in several spatio-velocity, X-ray profile, and stellar population studies of the Coma cluster (Biviano et al. 1996; Colless & Dunn 1996; Briel et al. 2001; Neumann et al. 2003; Adami et al. 2005; Smith et al. 2009, 2012, etc.).

The four UDGs from our outer mask have a mean radial velocity of $\sim 7630 \text{ km s}^{-1}$, comparable with the recession velocity of NGC 4839, i.e. $\sim 7360 \text{ km s}^{-1}$. Likewise, the four UDGs from the D16 mask have a mean radial velocity of $\sim 6835 \text{ km s}^{-1}$, similar to the mean velocity of their neighbouring galaxies. Within the cluster core, the mean radial velocity of the UDGs is $\sim 7020 \text{ km s}^{-1}$, comparable to the systemic velocity of the cluster (6943 km s^{-1}), while they have a velocity dispersion of $\sim 1480 \text{ km s}^{-1}$. NED cluster galaxies within the cluster core, on the other hand, have a mean radial velocity of $\sim 6910 \text{ km s}^{-1}$ and a velocity dispersion of $\sim 1110 \text{ km s}^{-1}$. Outside the cluster core, UDGs (including the literature UDGs) have a significantly elevated mean velocity of $\sim 7300 \text{ km s}^{-1}$. Note that these results for our UDGs do not change significantly if we include the two LSB galaxies in our analysis.

Taking all these results together, and bearing in mind our limited azimuthal coverage, it appears that Coma UDGs have kinematics consistent with their local neighbourhood. These suggest a formation origin that is closely linked with the gravitational potential within their local environment. We explore these in more detail next. However, due to the paucity of the presently available UDG RV data and their azimuthal incompleteness, we defer a cluster-wide comparison of their kinematics with the various galaxy subpopulations until more kinematics data become available.

²<http://ned.ipac.caltech.edu/>

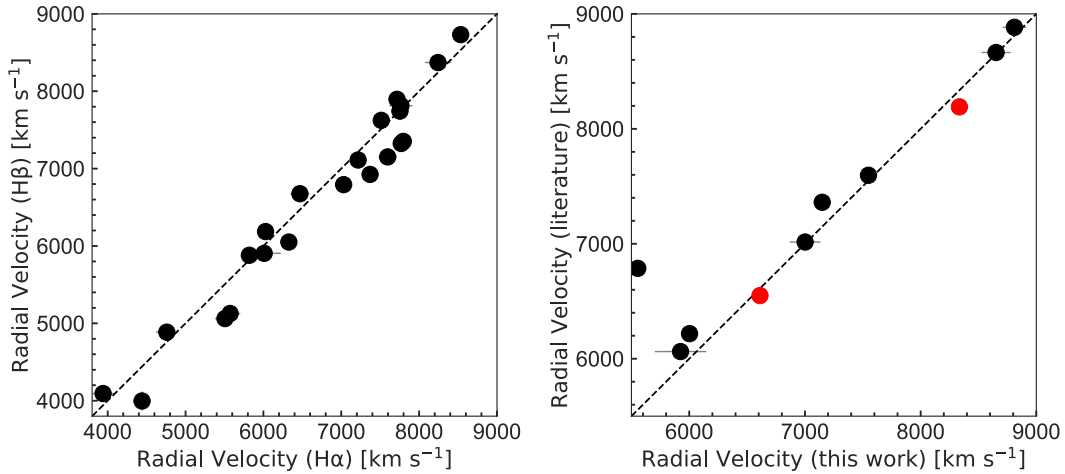


Figure 5. *Left:* Comparison of radial velocities obtained around the $H\beta$ - and $H\alpha$ -spectroscopic features. *Right:* Comparison of radial velocities obtained in this work with measurements available in the literature. The significantly deviant measurement is due to bad wavelength calibration in our spectral data for GMP3298, where only the $H\alpha$ -spectral range is available. The red points are UDGs Yagi 093 and Yagi 418 from Ruiz-Lara et al. (2018).

To further investigate the impact of the local environment on present-day UDGs within the cluster environment, we expand our parameter space, exploring their optical colours as a function of clustercentric radii. We also compare our UDGs with a sample of co-spatial, well-studied relatively high surface brightness (HSB) dwarf galaxies from Smith et al. (2009). Optical $B - R$ colours are directly available for 13 of the 25 UDGs as published in Y16, which they obtained from Yamanoi et al. (2012). Also, a few of the remaining spectroscopically confirmed UDGs, especially at large radii, have stellar population parameters available in the literature, from which we can infer their $B - R$ colour in line with the stellar population predictions from Vazdekis et al. (2015). We have also done a match of the Coma galaxies with radial velocities available in NED with the SDSS DR14 catalogue in order to obtain their SDSS $g - r$ optical colours. All the HSB dwarf galaxies from Smith et al. (2009) have SDSS $g - r$ colours. To convert the SDSS $g - r$ colours into Subaru filter system $B - R$, we extracted transformation equations from fig. 3 in Yamanoi et al. (2012) based on stars with colour measurements common to both studies. The transformation equation we use is $B - R = 1.4(g - r) + 0.05$.

From Fig. 7, UDGs within the cluster core with $B - R < 0.9$ – the average colour of Coma UDGs (Koda et al. 2015) – have an elevated mean absolute relative radial velocity of $\sim 1475 \pm 760 \text{ km s}^{-1}$, while redder UDGs have a lower mean absolute relative radial velocity of $\sim 970 \pm 900 \text{ km s}^{-1}$. Given the small size of our spectroscopic UDG sample, we ask if these mean velocities are significantly different. Using Welch’s t -test, we are not able to reject the null hypothesis that the mean velocities are identical (p -values for the bluer and redder UDGs are 0.39 and 0.47, respectively). We find that we would need to improve our Coma UDG spectroscopic sample by at least a factor of five to confirm any significant difference between the mean velocities of the bluer and redder UDGs at a p -value < 0.05 level, assuming identical velocity distributions as we have reported here. It should also be noted that the 3D clustercentric radii of some of these UDGs may be further away from the cluster centre due to projection effects.

Outside the cluster core, where the effects of projection are reduced, we only have two confirmed UDGs with observed colours, although we have also inferred the $B - R$ colours of the three UDGs from Gu et al. (2017). The very blue UDG not shown in Fig. 7 is

DF40 (also Yagi 507 in Y16) from Kadowaki et al. (2017). It has a $B - R$ colour of 0.5, and it is part of their spectral stack that they judged to be very old and metal poor. One of our targets without radial velocity measurement due to poor SNR, Yagi 774, also has a $B - R$ colour of 0.68. As shown in Fig. 7, most Coma UDGs in the outskirts that are yet to be spectroscopically confirmed have similar blue colours. However, due to the dearth of optical colours in the cluster outskirts and the peculiar effects from the NGC 4839 substructure, the true nature of the colour trend in the cluster outskirts is rather vague, though it appears that UDGs are preferentially bluer in the cluster outskirts. At this stage, the currently available data are simply not good enough to establish a significant radial and/or velocity trend with colour in the cluster outskirts, though there are hints of a possible velocity sequence, at least within the cluster core, such that slower moving UDGs, relative to the cluster, are redder in optical colours.

Next, we investigate possible correlations between UDG sizes, radial velocities, and their projected locations within the Coma cluster as shown in Fig. 8. Lisker et al. (2009) had already reported a link between the radial velocities of nucleated Virgo cluster dwarfs and their structural properties. They observed that slower moving dwarfs are rounder and predominantly on circular orbits, unlike the faster moving dwarfs that were found to be flatter and typically on eccentric orbit – a clear indicator of late infall. Román & Trujillo (2017b) also recently proposed an evolutionary scenario for UDGs based on their study of UDGs in field environments. They found that redder field UDGs are smaller, preferentially found near the group centres, and have been in their group environments longer, i.e. consistent with being they are early infalls. They attributed their observed size trend to the effect of physical processes such as ram-pressure stripping or tidal stripping that leads to end products that are smaller.

From Fig. 8, if we consider the entire spectroscopically confirmed UDG dataset, we do not find any clear trend between the sizes, projected locations within the cluster, and kinematics of Coma cluster UDGs. It is neither obvious that smaller UDGs are preferentially located in the cluster core nor is it evident that slowly moving UDGs are smaller. However, if we consider only the UDGs within the cluster core, we find significant anticorrelation between UDG sizes and their absolute velocities, with a Spearman rank

Table 1. Ultradiffuse galaxy sample and other targets from the Coma cluster studied in this work. The horizontal lines separate UDGs from LSB galaxies and from filler, non-UDGs, respectively. The galaxy IDs, coordinates, R -band magnitudes, $B - R$ colours, surface brightnesses, and sizes for the UDGs and LSB galaxies are from the Yagi et al. (2016) catalogue. Masks ‘C’ and ‘O’ denote the central and outer masks, respectively, described in Section 2.2, while mask ‘D16’ is described in Section 2.4. SNR is measured around the $H\beta$ or $H\alpha$ region, as described in text. The galaxy IDs shown for the filler objects are mostly from the SDSS DR14 (Abolfathi et al. 2017) catalogue except when they have also been catalogued in Godwin, Metcalfe & Peach (1983). We have translated their SDSS- r band magnitudes into Subaru- R band using equation 2 and table 1 from Yagi et al. (2013). The sizes shown for the filler galaxies are from single component Sérsic fits to their Subaru- R band image. Only the filler objects for which we have successfully measured radial velocities are shown in the table. In the ‘Add. IDs’ column, we list the IDs of our galaxy sample as presented in Godwin et al. (1983) and van Dokkum et al. (2015).

Galaxy	RA (J2000)	Dec. (J2000)	Mask	R (mag)	$B - R$ (mag)	μ_0 (mag arcsec $^{-2}$)	R_e (kpc)	SNR	Vel (km s $^{-1}$)	Add. IDs
Yagi090	13:00:20.37	+27:49:24.0	C	20.3	0.86	24.4	1.92	<5	–	–
Yagi093	13:00:20.61	+27:47:12.3	C	18.9	0.96	23.6	3.49	15.3	6611±137	DF26, GMP2748
Yagi098	13:00:23.20	+27:48:17.1	C	19.6	0.96	24.9	2.30	20.8	5980±82	–
Yagi263	12:59:15.33	+27:45:14.8	C	20.8	1.04	24.3	2.04	5.7	6695±147	–
Yagi275	12:59:29.89	+27:43:03.1	C	19.2	0.92	23.5	2.93	15.2	4847±149	GMP3418
Yagi276	12:59:30.46	+27:44:50.4	C	19.6	0.9	24.0	2.25	13.9	7343±102	DF28
Yagi285	12:59:48.72	+27:46:39.0	C	19.7	1.0	24.8	3.88	12.4	6959±121	DF25
Yagi364	12:59:23.85	+27:47:27.2	C	20.0	0.95	25.2	2.42	15.8	7068±90	DF23
Yagi392	12:59:56.17	+27:48:12.8	C	20.7	0.97	24.0	1.46	7.3	7748±161	–
Yagi398	13:00:00.41	+27:48:19.7	C	20.1	0.96	23.6	1.34	19.5	4180±167	–
Yagi417	13:00:12.10	+27:48:23.5	C	21.4	0.83	24.9	1.62	8.5	9038±179	–
Yagi418	13:00:11.71	+27:49:41.0	C	20.4	0.93	23.9	1.57	16.0	8335±187	–
Yagi762	12:55:55.40	+27:27:35.9	O	20.5	–	24.5	1.97	5.5	7188±127	DF36
Yagi764	12:55:56.65	+27:30:17.6	O	20.0	–	23.5	2.44	7.2	7050±115	–
Yagi767	12:55:59.15	+27:25:53.4	O	20.6	–	24.3	2.37	<5	–	–
Yagi771 ^a	12:56:05.38	+27:30:18.2	O	22.2	–	24.8	1.60	5.4	11007±192	–
Yagi774	12:56:12.95	+27:32:50.3	O	20.6	0.68	25.9	3.07	<5	–	–
Yagi776	12:56:14.15	+27:33:19.7	O	20.2	0.81	24.0	2.3	7.4	8473±81	–
Yagi781	12:56:28.29	+27:36:11.5	O	20.8	–	24.2	1.64	<5	–	–
Yagi782	12:56:28.41	+27:37:06.3	O	20.1	–	24.6	2.8	<5	–	DF32
Yagi786	12:56:35.20	+27:35:07.0	O	19.4	–	23.5	2.34	6.6	7810±141	–
Yagi012 ^b	13:01:05.30	+27:09:35.1	D16	20.6	–	23.7	1.57	4.1	6473±33	DFX2
Yagi266	12:59:20.25	+27:46:33.3	C	22.6	–	25.7	0.87	5.2	6366±139	–
Yagi413	13:00:10.19	+27:49:19.8	C	22.2	0.84	24.2	0.85	9.7	5014±196	–
Yagi772	12:56:09.07	+27:34:16.2	O	21.7	–	24.7	1.21	<5	–	–
GMP2749	13:00:20.48	+27:48:17.0	C	18.4	–	–	1.59	18.8	5846±74	–
GMP2800	13:00:17.55	+27:47:03.9	C	16.7	–	–	2.92	21.8	7001±132	–
GMP2923	13:00:08.05	+27:46:24.1	C	16.8	–	–	2.09	9.8	8652±125	–
GMP2945	13:00:06.29	+27:46:32.9	C	14.6	–	–	2.63	24.3	6091±66	–
GMP3037	12:59:59.39	+27:47:55.8	C	19.1	–	–	0.76	11.6	13938±142	–
GMP3071	12:59:56.11	+27:44:46.7	C	16.1	–	–	1.39	13.9	8810±99	–
GMP3519	12:59:22.94	+27:43:24.5	C	18.7	–	–	1.88	19.2	4062±167	–
GMP3298	12:59:37.83	+27:46:36.6	C	15.3	–	–	4.27	18.5	5554±41	–
GMP3493	12:59:24.93	+27:44:19.9	C	14.9	–	–	1.38	23.2	6001±80	–
J125924.95+274529.0 ^c	12:59:24.95	+27:45:29.0	C	21.9	–	–	0.82	6.2	5420±166	–
J125944.10+274607.5	12:59:44.11	+27:46:07.6	C	19.2	–	–	0.91	22.9	6109±127	–
J125942.65+274658.8	12:59:42.65	+27:46:59.4	C	20.2	–	–	1.36	30.1	5418±163	–
J125948.33+274547.6	12:59:48.37	+27:45:48.2	C	21.2	–	–	1.37	9.6	8039±109	–
J125939.09+274557.5	12:59:39.10	+27:45:57.5	C	20.1	–	–	0.88	15.7	7791±164	–
GMP5357	12:56:34.86	+27:37:38.6	O	18.5	–	–	1.98	13.2	7239±97	–
GMP5455	12:56:24.46	+27:32:18.4	O	17.8	–	–	1.33	18.4	7413±85	–
GMP5465	12:56:23.36	+27:32:38.5	O	17.3	–	–	0.87	17.5	7149±50	–
J125638.44+273415.3	12:56:38.44	+27:34:15.3	O	17.4	–	–	1.68	8.8	7549±49	–
J125623.18+273358.1	12:56:23.18	+27:33:58.1	O	19.2	–	–	0.68	5.0	5655±69	–
J125608.14+272906.5	12:56:08.14	+27:29:06.5	O	21.7	–	–	1.07	5.1	6946±143	–
J125620.09+273623.7	12:56:20.09	+27:36:23.7	O	20.7	–	–	0.97	13.3	6208±87	–
J125610.30+273104.4	12:56:10.30	+27:31:04.4	O	22.7	–	–	0.44	5.2	6333±182	–
J125603.20+273213.4	12:56:03.20	+27:32:13.4	O	21.4	–	–	0.57	8.7	3434±150	–
J130110.36+265636.4	13:01:10.36	+26:56:36.4	D16	18.3	–	–	0.53	10.6	7916±75	–
J130103.69+265717.2	13:01:03.69	+26:57:17.2	D16	19.3	–	–	0.38	14.6	7719±40	–
J130109.88+265839.2	13:01:09.88	+26:58:39.2	D16	21.3	–	–	0.49	6.2	9028±25	–
J130108.86+270006.3	13:01:08.86	+27:00:06.3	D16	22.7	–	–	0.40	4.8	5272±40	–
J130104.75+270035.0	13:01:04.75	+27:00:35.0	D16	18.1	–	–	0.71	16.2	4563±67	–
J130111.71+270136.9	13:01:11.71	+27:01:36.9	D16	21.2	–	–	0.65	7.7	4160±27	–
J130113.58+270158.8	13:01:13.58	+27:01:58.8	D16	22.0	–	–	0.4	8.8	8015±37	–
J130115.54+270348.0	13:01:15.54	+27:03:48.0	D16	19.9	–	–	0.47	12.6	7762±58	–
J130108.49+270817.7	13:01:08.49	+27:08:17.7	D16	20.7	–	–	0.86	7.7	5045±34	–
J130109.18+271110.3	13:01:09.18	+27:11:10.3	D16	21.0	–	–	0.49	6.3	9957±29	–
J130117.24+271104.5	13:01:17.24	+27:11:04.5	D16	21.4	–	–	0.34	4.2	5058±20	–
J130124.47+271129.5	13:01:24.47	+27:11:29.5	D16	22.5	–	–	0.47	6.6	8428±44	–

^aThe size we report for Yagi 771 is updated to correspond to a distance of ~ 160 Mpc and the radial velocity shown. ^bYagi012 is the ultradiffuse galaxy from the D16 mask with radial velocity not published in the literature. ^cJ125924.95+274529.0 is not detected in SDSS DR14 but has photometry available in the catalogue of Adami et al. (2006).

correlation coefficient of -0.64 and a p -value of 0.03 . The same trend is not observed in the more compact, co-spatial HSB dwarf galaxy sample. This finding, that slowly moving UDGs within the cluster core are bigger (and vice versa), contradicts the finding of

Román & Trujillo (2017b) obtained in less-dense environment. Our result might be an indication that within the cluster core, where the gravitational potential is deeper, physical processes such as tidal heating (Boselli & Gavazzi 2006; Safarzadeh & Scannapieco 2017;

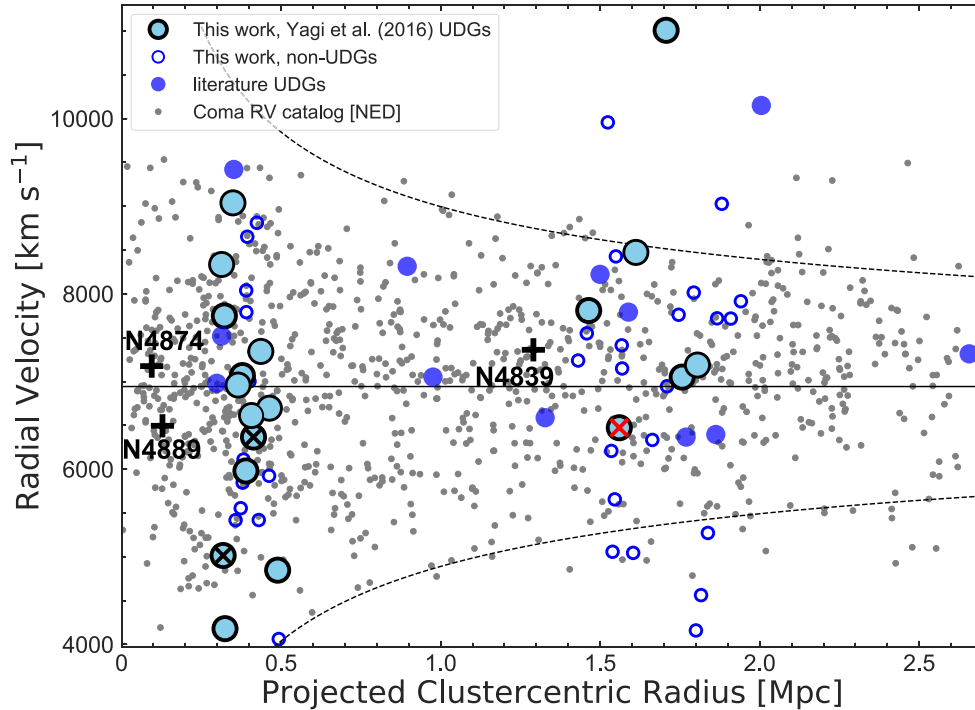


Figure 6. Clustercentric radial velocity distribution of galaxies in the Coma cluster. Cluster galaxies with radial velocity measurements available in the literature are shown as grey dots. The black solid line is the recessional velocity of the Coma cluster, while the dashed curves shows the velocity limits consistent with the virial mass reported in Kubo et al. (2007). We have marked the three most luminous galaxies in the Coma cluster, i.e. NGC 4874, NGC 4889, and NGC 4839. UDGs from Yagi et al. (2016) for which we have measured radial velocities are shown as the skyblue circles with black edges. The blue open circles are the non-UDGs for which we have also obtained radial velocities. The blue circles without black edges are UDGs with radial velocity measurements from the literature. Yagi012, the UDG from the D16 mask, is marked with a red cross, while the LSB galaxies (see Table 1) are marked with black crosses. Yagi 771, one of our target UDGs, is consistent with being a cluster background galaxy.

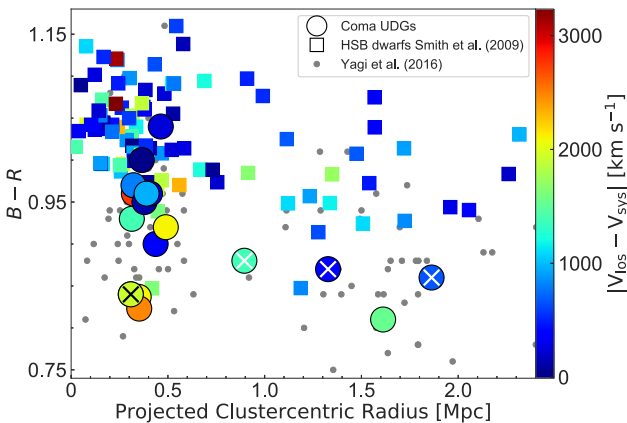


Figure 7. Optical colour as a function of clustercentric radii for spectroscopically confirmed galaxies in the Coma cluster. UDGs without colour information from Yamanoi et al. (2012) and/or stellar population parameters in the literature are shown as grey dots. The LSB galaxy (Yagi 774 is marked with a black cross, while UDGs with inferred colours (from Gu et al. 2017) have been marked with white crosses. We do not show DF40 at ~ 1.5 Mpc with $B - R = 0.5$ in order to highlight the trend within the cluster core. Co-spatial dwarf galaxies from Smith et al. (2009) are also shown for comparison, and they are, on average, redder than UDGs at any radii. All galaxies have been colour coded by their absolute line-of-sight velocities relative to the cluster. Within the cluster core, UDGs with higher absolute relative velocity are bluer.

Carleton et al. 2018) are relatively more important in the evolution of UDGs, making them bigger.

4.2 Are UDGs late infalls into the cluster?

We now explore the origins of UDGs within the Coma cluster with a velocity phase-space diagram. We combine the spatial, line-of-sight velocity, and optical colour information of the spectroscopically confirmed UDGs in the modified phase-space plot shown in Fig. 9. The horizontal axis, $R_{\text{proj}}/R_{200} \times |V_{\text{los}} - V_{\text{sys}}|/\sigma$, is now a proxy for the accretion epoch (see Haines et al. 2012; Noble et al. 2013; Rhee et al. 2017, etc.). For easy referencing, hereafter, we will refer to this quantity as *infall time*, although we note that it is a dimensionless quantity. The horizontal axis is a proxy for accretion epoch because in velocity phase space, $R_{\text{proj}} \times V_{\text{los}}$ is constant along ‘chevron’-shaped caustics and may be used to identify infalling or virialized groups within the cluster. In Fig. 9, galaxies along any vertical line share similar accretion epochs and as such, we can qualitatively infer the infall times of our UDG sample relative to the three brightest galaxies within the Coma cluster. Galaxies with smaller $R_{\text{proj}} \times V_{\text{los}}$ have been in the cluster longer on average, and vice versa, such that NGC 4874 is nearest the centre of the cluster potential, and NGC 4839 is a relatively late infall. One important caveat that should be borne in mind when interpreting our modified phase-space diagram is the effect of projection that makes the qualitative *infall time*, we report here, lower limits. Also, note that early (late) infalls are not necessarily limited to the cluster core (outskirts). According to the cosmological simulations of Rhee et al. (2017), these late and early

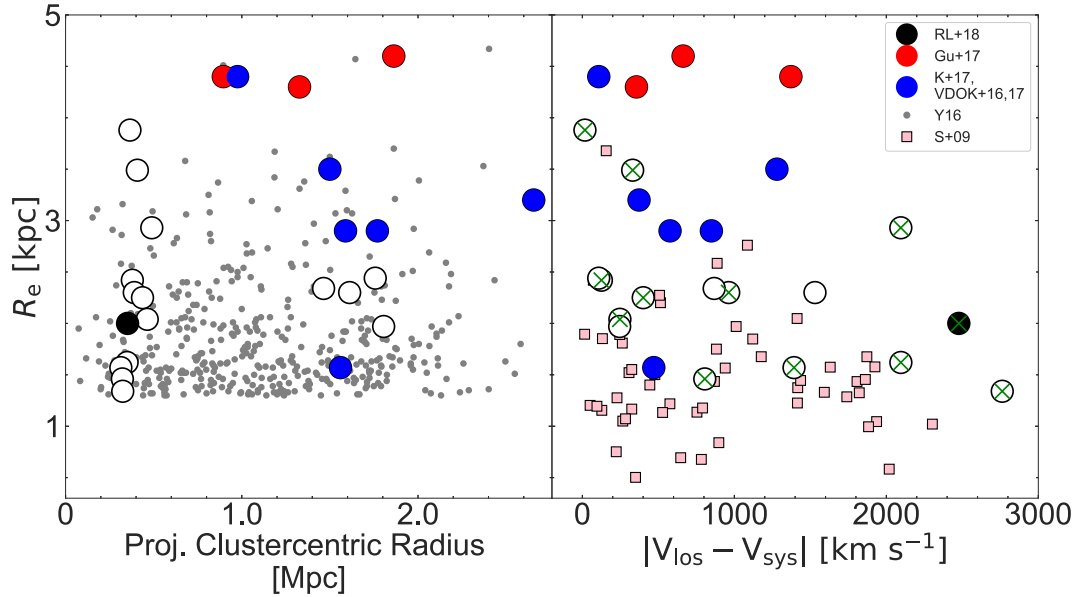


Figure 8. Galaxy size as a function of clustercentric radii and absolute relative radial velocities for Coma cluster UDGs. UDGs have been colour-coded as shown in the plot legend with Gu+17, RL+18, K+17, and VDOK+16,17 being Yagi et al. (2016) UDGs from Gu et al. (2017), Ruiz-Lara et al. (2018), Kadowaki et al. 2017, van Dokkum et al. 2016, 2017, respectively. The grey dots are UDGs that have not been spectroscopically confirmed. UDGs within the cluster core are marked with green crosses in the right-hand panel, and we also compare with cluster core dwarf galaxies from Smith et al. (2009).

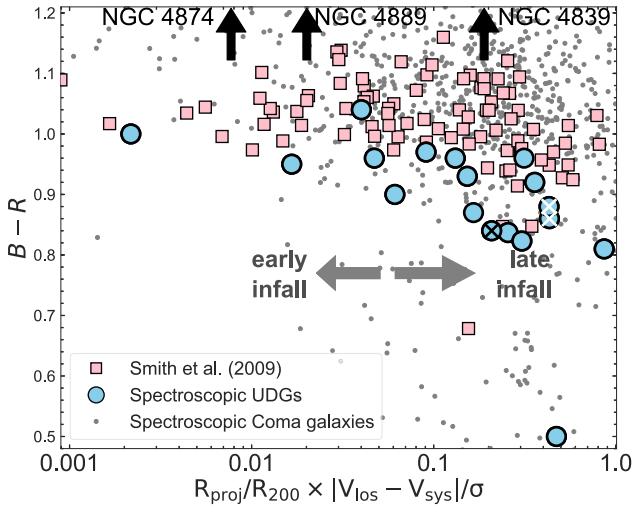


Figure 9. Modified phase-space diagram showing optical colour of Coma galaxies as a function of their qualitative infall time. The horizontal axis is a proxy for the infall time of galaxies into the Coma cluster. The upward pointing arrows represent the infall times of the three brightest cluster galaxies as shown in the plot. We have also included the HSB dwarf galaxies from Smith et al. (2009) in the diagram for comparison. As in previous Figures, the UDGs with inferred optical $B-R$ colours (from Gu et al. 2017) have been marked with white crosses, while the LSB galaxy is marked with a black cross. The grey arrows point, where early and late infalls may be found in the modified phase space.

infalls are expected, on average, to have been in a Coma-like cluster for ~ 2 and ~ 8 Gyr, respectively. Lastly, we note that while the modified phase space gives extra constraint on the origins of UDGs via their infall times, it does not necessarily imply that all UDGs have an ex-situ origin, as we discuss next.

From Fig. 9, a clear picture emerges, where the bluest UDGs in our sample are consistent with being late infalls, in agreement with the evolutionary scenario for UDGs in group environments (Román & Trujillo 2017b). These bluer UDGs are typically characterized by high absolute line-of-sight velocities and are smaller on average (within the cluster core). We note that most of these late infalls are not co-spatial with NGC 4839 despite having similar accretion epochs. There is thus evidence that the NGC 4839 subgroup may not be the sole driver of the trends we observed earlier in the cluster outskirts, although there is a noticeable overdensity of UDGs and dwarfs with accretion epochs similar to NGC 4839. Most of the UDGs in the sample we have studied in this paper therefore share a similar late infall origin with their dwarf galaxy neighbours.

However, it is also clear from Fig. 9 that not all of our UDGs are consistent with being late infalls, hence the origin of UDGs within the Coma cluster is best described as diverse. The accretion epochs of some UDGs in our sample are comparable with NGC 4874 and NGC 4889 that suggests that they have been in the cluster environment for longer periods (≥ 8 Gyr). From our modified phase space, the UDGs that are most likely to be early infalls (assuming they were not formed *in situ* at earlier epochs) are Yagi 285, Yagi 364, DF08, and Yagi 093. In Paper II, we report a stellar age of ~ 8 Gyr for Yagi 093, which may now be undergoing some disruption, consistent with the expected infall time from Rhee et al. (2017). It is possible that the progenitors of these early-infall UDGs were accreted bluer at earlier epochs and have become redder as they evolved within the cluster environment. It is also possible that they are failed galaxies formed in relatively massive halos that experienced star formation quenching at earlier epochs. In Paper II, we perform a detailed study of the stellar population properties of our UDG sample and find further evidence that while some of them have stellar population properties consistent with a late infall origin, similar to their normal dwarf galaxy neighbours, some of them may be failed, primordial galaxies, or early infalls.

5 SUMMARY AND PROSPECTS

In this work, we have spectroscopically confirmed the cluster membership of 16 new UDGs within the Coma cluster using Keck/DEIMOS data. This brings the total number of UDGs within the Coma cluster from the Yagi et al. (2016) catalogue with line-of-sight velocities to 25. With this modest kinematics sample, we have performed a pilot exploration of UDGs in velocity phase space with the aim of understanding their origins. We find evidence that are as follows:

- (i) Most (~95 per cent) UDGs in the LSB catalogue of Yagi et al. (2016) are members of the Coma cluster.
- (ii) The kinematics of UDGs are consistent with other galaxies in their vicinity.
- (iii) Within the cluster core, UDGs with higher absolute velocities have bluer optical colours and are smaller, unlike their slowly moving counterparts that are redder.
- (iv) Using the modified velocity phase space, we find evidence of a diverse origin for Coma cluster UDGs, similar to normal dwarf galaxies. Some UDGs in our sample are consistent with being late infalls into the cluster (at epochs comparable to that of NGC 4839), while some UDGs may have been in the cluster for as long as the most luminous galaxies within the cluster core. These early infalls may also be failed galaxies that experienced early star formation quenching.

The results presented in this pilot work show that while UDGs may or may not be spatially associated with visible kinematic substructures in cluster environments, their velocity distribution shows signs that are consistent with an infall origin of progenitors, over multiple episodes of accretion, similar to their co-spatial dwarf galaxy neighbours. These progenitors, which are significantly bluer, acquire radial velocities corresponding to the mass of the cluster at accretion as they are accelerated towards the cluster centre, become redder and bigger, on average, as they evolve within the harsh cluster environment via a complex interplay of physical processes such as tidal heating, ram-pressure stripping, and tidal stripping. Based on the currently available data, Coma cluster UDGs are best described as having a diverse origin with some of them consistent with being late or early infalls or even *in situ* formed, failed galaxies. As more spectroscopic data become available from different parts of the cluster, it would be interesting to see how Fig. 9 evolves, and to further investigate the relationship between the structural properties and kinematics of cluster UDGs relative to field UDGs, as this might give clearer indication of the dominant physical processes at play. Deep spectroscopy of UDGs in the cluster outskirts as well as in the field environments is definitely needed to properly understand their true origin(s). Lastly, it may now be possible to identify infalling galaxies that are being transformed into UDGs with the modified phase-space diagram.

ACKNOWLEDGEMENTS

We wish to thank the referee for constructive comments that have improved the quality of this manuscript. We wish to thank Pieter van Dokkum for providing the D16 DEIMOS mask data. This work was supported by NSF grants AST-1211995 and AST-1616598. AJR was supported by NSF grant AST-1515084 and as a Research Corporation for Science Advancement Cottrell Scholar. AFM and DAF thank the ARC for financial support via DP160101608. SB acknowledges the support of the AAO PhD Topup Scholarship.

MBS acknowledges financial support from the Academy of Finland, grant 311438.

The data presented herein were obtained at the W. M. Keck Observatory, which is operated as a scientific partnership among the California Institute of Technology, the University of California, and the National Aeronautics and Space Administration. The Observatory was made possible by the generous financial support of the W.M. Keck Foundation. The authors wish to recognize and acknowledge the very significant cultural role and reverence that the summit of Mauna kea has always had within the indigenous Hawaiian community. We are most fortunate to have the opportunity to conduct observations from this mountain.

REFERENCES

- Abolfathi B. et al., 2017, *ApJS*, 235, 42
 Adami C., Biviano A., Durret F., Mazure A., 2005, *A&A*, 443, 17
 Adami C. et al., 2006, *A&A*, 451, 1159
 Amorisco N. C., Monachesi A., Agnello A., White S. D. M., 2018, *MNRAS*, 475, 4235
 Beasley M. A., Trujillo I., 2016, *ApJ*, 830, 23
 Bertschinger E., 1985, *ApJS*, 58, 39
 Binney J., Tremaine S., 2008, *Galactic Dynamics*, 2nd edn. Princeton Univ. Press, Princeton, NJ
 Biviano A., Durret F., Gerbal D., Le Fevre O., Lobo C., Mazure A., Slezak E., 1996, *A&A*, 311, 95
 Boselli A., Gavazzi G., 2006, *PASP*, 118, 517
 Briel U. G. et al., 2001, *A&A*, 365, L60
 Burkert A., 2017, *ApJ*, 838, 93
 Cardiel N., 1999, PhD thesis, Univ. Complutense de Madrid
 Carleton T., Errani R., Cooper M., Kaplinghat M., Peñarrubia J., 2018, preprint ([arXiv:1805.06896](https://arxiv.org/abs/1805.06896))
 Chan T. K., Kereš D., Wetzel A., Hopkins P. F., Faucher-Giguère C.-A., El-Badry K., Garrison-Kimmel S., Boylan-Kolchin M., 2017, *MNRAS*, 478, 906
 Colless M., Dunn A. M., 1996, *ApJ*, 458, 435
 Conselice C. J., Gallagher III J. S., Wyse R. F. G., 2001, *ApJ*, 559, 791
 Cooper M. C., Newman J. A., Davis M., Finkbeiner D. P., Gerke B. F., 2012, *Astrophysics Source Code Library*, record ascl:1203.003
 Di Cintio A., Brook C. B., Dutton A. A., Macciò A. V., Obreja A., Dekel A., 2017, *MNRAS*, 466, L1
 Ferré-Mateu A. et al., 2018, *MNRAS*, in press
 Godwin J. G., Metcalfe N., Peach J. V., 1983, *MNRAS*, 202, 113
 Gu M. et al., 2017, *ApJ*, 859, 37
 Haines C. P. et al., 2012, *ApJ*, 754, 97
 Haines C. P. et al., 2015, *ApJ*, 806, 101
 Janssens S., Abraham R., Brodie J., Forbes D., Romanowsky A. J., van Dokkum P., 2017, *ApJ*, 839, L17
 Kadowaki J., Zaritsky D., Donnerstein R. L., 2017, *ApJ*, 838, L21
 Koda J., Yagi M., Yamanoi H., Komiyama Y., 2015, *ApJ*, 807, L2
 Kubo J. M., Stebbins A., Annis J., Dell’Antonio I. P., Lin H., Khiaabanian H., Frieman J. A., 2007, *ApJ*, 671, 1466
 Lisker T. et al., 2009, *ApJ*, 706, L124
 Mahajan S., Mamon G. A., Raychaudhury S., 2011, *MNRAS*, 416, 2882
 Makarov D., Prugniel P., Terekhova N., Courtois H., Vauglin I., 2014, *A&A*, 570, A13
 Mamon G. A., Sanchis T., Salvador-Solé E., Solanes J. M., 2004, *A&A*, 414, 445
 Martínez-Delgado D. et al., 2016, *AJ*, 151, 96
 Mendelin M., Binggeli B., 2017, *A&A*, 604, A96
 Neumann D. M., Lumb D. H., Pratt G. W., Briel U. G., 2003, *A&A*, 400, 811
 Noble A. G., Webb T. M. A., Muzzin A., Wilson G., Yee H. K. C., van der Burg R. F. J., 2013, *ApJ*, 768, 118
 Oman K. A., Hudson M. J., Behroozi P. S., 2013, *MNRAS*, 431, 2307
 Pandya V. et al., 2017, *ApJ*, 858, 29

- Rhee J., Smith R., Choi H., Yi S. K., Jaffé Y., Candlish G., Sánchez-Jánssen R., 2017, *ApJ*, 843, 128
- Román J., Trujillo I., 2017a, *MNRAS*, 468, 703
- Román J., Trujillo I., 2017b, *MNRAS*, 468, 4039
- Rong Y., Guo Q., Gao L., Liao S., Xie L., Puzia T. H., Sun S., Pan J., 2017, *MNRAS*, 470, 4231
- Ruiz-Lara T. et al., 2018, *MNRAS*, 478, 2034
- Safarzadeh M., Scannapieco E., 2017, *ApJ*, 850, 99
- Sarazin C. L., 1986, *Rev. Mod. Phys.*, 58, 1
- Shi D. D. et al., 2017, *ApJ*, 846, 26
- Smith R. J., Lucey J. R., Hudson M. J., Allanson S. P., Bridges T. J., Hornschemeier A. E., Marzke R. O., Miller N. A., 2009, *MNRAS*, 392, 1265
- Smith R. J., Lucey J. R., Price J., Hudson M. J., Phillipps S., 2012, *MNRAS*, 419, 3167
- Spekkens K., Karunakaran A., 2017, *ApJ*, 855, 28
- Tonry J., Davis M., 1979, *AJ*, 84, 1511
- van der Burg R. F. J., Muzzin A., Hoekstra H., 2016, *A&A*, 590, A20
- van der Burg R. F. J. et al., 2017, *A&A*, 607, A79
- van Dokkum P. G. et al., 2015, *ApJ*, 804, L26
- van Dokkum P. et al., 2016, *ApJ*, 828, L6
- van Dokkum P. et al., 2017, *ApJ*, 844, L11
- Vazdekis A. et al., 2015, *MNRAS*, 449, 1177
- Vazdekis A., Koleva M., Ricciardelli E., Röck B., Falcón-Barroso J., 2016, *MNRAS*, 463, 3409
- Vijayaraghavan R., Gallagher J. S., Ricker P. M., 2015, *MNRAS*, 447, 3623
- Yagi Nao M. S., Yamanoi H., Furusawa H., Nakata F., Komiyama Y., 2013, *PASJ*, 65, 22
- Yagi M., Koda J., Komiyama Y., Yamanoi H., 2016, *ApJS*, 225, 11
- Yamanoi H. et al., 2012, *AJ*, 144, 40

This paper has been typeset from a $\text{\TeX}/\text{\LaTeX}$ file prepared by the author.